$(CO)_3PPh_3]Si_6Me_{10}[Fe(CO)_2Cp]$. ^{29}Si NMR (ppm): −3.80 (d); −28.65 (d); −27.06 (d); −16.04 (s). ^{13}C NMR (ppm): 216.14; 201.50 (d); 135.79; 133.89; 133.74; 131.00; 129.36; 129.26; 82.81; 2.79; 2.47; −0.38; −0.49; −0.82. ^1H NMR (ppm): 7.61 (m), 6.99 (m) (15 H); 4.29 (s) (5 H); 0.70, 0.49, 0.35 (s) (30 H). ^{31}P NMR (ppm): 58.67 ($^2J_{Si-P}$ = 18.24 Hz, $^3J_{Si-P}$ = 1.21 Hz, $^4J_{Si-P}$ = 4.45 Hz). IR (cm^{-1}): 1992, 1973, 1941 (ν_{C-O}). Mp: 151–155 °C dec. Anal. Calcd/Found: C, 50.67/50.1; H, 5.55/5.7; Fe, 6.20/6.1; Co, 6.54/6.7.

1,4-Dibromodecamethylcyclohexasilane. $CHBr_3$ (10 g, 40 mmol) and $Si_6Me_{10}H_2$ (5 g, 15.5 mmol) were refluxed in 20 mL of toluene until no more $Si_6Me_{10}H_2$ could be detected by GC analysis. Toluene and excess $CHBr_3$ were removed under vacuum. Sublimation of the white solid residue at 100 °C (10^{-3} bar) yielded 7 g (95%) of white crystalline $Si_6Me_{10}Br_2$. ^{29}Si NMR (ppm): 9.61/7.93; −39.88/−39.73.

1,4-Bis[tricarbonyl(triphenylphosphino)cobalt]decamethylcyclohexasilane. $Na[Co(CO)_3PPh_3]$ (1.32 g, 3.0 mmol) and $Si_6Me_{10}Cl_2$ (0.6 g, 1.5 mmol) were stirred in 250 mL of THF for about 12 h at room temperature until the ν_{C-O} at 1932, 1856, and 1810 cm^{-1} disappeared in the IR spectra. The solvent was removed under vacuum, and the dark yellow residue was suspended in 50 mL of benzene. After filtration through a Celite pad and concentration of the solution to 15 mL, yellow crystals precipitated. Those were filtered off, rinsed with 30 mL of hexane, and dried under vacuum. Yield: 0.6 g, 35%. ^{29}Si NMR (ppm): −4.10/−4.54 (d); −30.49/−31.83 (d). ^1H NMR (ppm): 7.61 (m), 6.98 (m) (30 H); 1.12, 0.75, 0.66 (30 H). ^{13}C NMR (ppm): 201.61 (d); 135.898; 133.877; 133.717; 130.951; 129.313; 129.189; −1.180; −1.69; −2.76; −3.04. ^{31}P NMR (ppm): 58.761 ($^2J_{Si-P}$ = 18.43/18.58 Hz; $^3J_{Si-P}$ < 0.8 Hz; $^4J_{Si-P}$ = 3.62/3.61 Hz). IR (cm^{-1}): 1947 (ν_{C-O}). Mp: 187–192 °C dec. Anal. Calcd/Found: C, 55.30/54.9; H, 5.59/5.4.

[Tricarbonyl(triphenylphosphino)cobalt]undecamethylcyclohexasilane. A 1.5-g (3.6-mmol) portion of $Si_6Me_{11}Br$ was dissolved in 40 mL of THF and the resultant mixture added at −50 °C to 1.6 g (3.6 mmol) of $Na[Co(CO)_3PPh_3]$ in 200 mL of THF. The reaction mixture was allowed to warm to room temperature and then stirred for 2 h. After evaporation of the solvent, the residue was extracted with 100 mL of pentane. The solution was concentrated until yellow crystals precipitated. Filtration at −30 °C gave 1.92 g (72%) of pure $Si_6Me_{11}Co(CO)_3PPh_3$. ^{29}Si NMR (ppm): −3.91 (d); −32.19 (d); −41.01 (d); −43.64 (s). ^{13}C NMR (ppm): 201.5 (d); 135.75; 135.186; 133.849; 133.71; 131.00; −1.745; −3.4; −4.34; −5.28; −5.527. ^1H NMR (ppm): 7.61 (m), 6.97 (m); 1.05 (d); 0.65; 0.61; 0.26. ^{31}P NMR (ppm): 58.57 ($^2J_{Si-P}$ = 18.51 Hz; $^3J_{Si-P}$ = 1.08 Hz; $^4J_{Si-P}$ = 4.06 Hz). Mp: 174–183 °C dec. Anal. Calcd/Found: C, 52.00/51.8; H, 6.55/6.4.

Acknowledgment. We are grateful to the Fond zur Förderung der wissenschaftlichen Forschung (Wien) for financial support and the Wacker Chemie, GmbH Burghausen, for the supply of silanes.

Solution and Solid-State Conformations of 5,5′-Bis(trimethylsilyl)-10,11-dihydro-5*H*-dibenzo[*b*,*f*]silepins

Lura D. Lange, Joyce Y. Corey,* and Nigam P. Rath

Department of Chemistry, University of Missouri—St. Louis, 8001 Natural Bridge Road, St. Louis, Missouri 63121

Received October 9, 1990

Three new 10,11-dihydro-5*H*-dibenzo[*b*,*f*]silepins have been synthesized. The structures of two of the silepins, 5,5′-bis(trimethylsilyl)-4,6-dimethyl-10,11-dihydro-5*H*-dibenzo[*b*,*f*]silepin (**2**) and 5,5′-bis(trimethylsilyl)-10,11-5*H*-dibenzo[*b*,*f*]silepin (**3**), have been solved by X-ray crystallography. Compound **2** crystallizes in the orthorhombic space group *Pccn* with $Z = 8$, $a = 14.888$ (10) Å, $b = 15.98$ (2) Å, and $c = 20.12$ (3) Å. Compound **3** crystallizes in space group $C2/c$ (monoclinic) with $Z = 4$, $a = 15.606$ (5) Å, $b = 16.061$ (5) Å, $c = 8.896$ (3) Å, and $\beta = 102.26$ (2)°. The structures were refined to $R(F) = 0.0540$ and 0.0553 and $R_w(F) = 0.0638$ and 0.0586 for 719 and 617 reflections for **2** and **3**, respectively. The ^1H NMR spectra indicate that **2** exhibits a unique conformational rigidity at room temperature, while the remaining two silepins are fully fluxional to temperatures of −90 °C (183 K). The ethano bridge region for **2** exhibits an AA′BB′ pattern at room temperature and coalescence to A_4 occurs at 80 °C (353 K). The dynamic process associated with **2** was analyzed by DNMR4 techniques and the free energy of activation (ΔG^*) is found to be 16 kcal/mol for the inversion of the central seven-membered ring. A comparison of the solid-state and solution structures of **2** and related molecules is also given.

Dibenzoheteroepins (**1**) with appropriate aminoalkyl side chains exhibit diverse biological activities in the central nervous system. Attempts have been made to develop

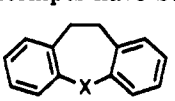

1

structure–activity relationships by using X-ray crystallography (solid state), nuclear magnetic resonance (solution studies), and computer-assisted molecular modeling.[1] Common functionalities such as an aromatic ring and an amine group appear to be important in the biological function of these compounds and the relationship of their relative positions have been analyzed.[2]

Frequently, structural studies have been simplified by consideration of only the parent tricycle in order to separate the conformational properties of the framework from those of the side chain. The tricyclic framework can exist in varied conformations as a result of the twist of the C(10)–C(11) bond (the ethano bridge) and changes in bend angles (e.g., dihedral angles between benzo group planes).

Since the solid-state conformation may not be the biologically active conformer, solution studies could provide models for molecules in a more physiologically relevant environment. The dibenzoheteroepin framework most frequently studied in solution is the azepine system (**1**, X

(1) (a) Bandolini, G.; Nicolini, M.; Tollenaere, J. P. *J. Crystallogr. Spectrosc. Res.* **1984**, *14*, 401. (b) Andrews, P. R.; Lloyd, E. J.; Martin, J. L.; Munro, S. L.; Sadek, M.; Wong, M. G. In *Molecular Graphics and Drug Design*; Burgen, A. S. V., Roberts, G. C. K., Tute, M. S., Eds.; Elsevier Science Publishers, B. V.: Amsterdam, 1986; Chapter 9.

(2) Lloyd, E. J.; Andrews, P. R. *J. Med. Chem.* **1986**, *29*, 453–462.

0276-7333/91/2310-3189$02.50/0

= NR), particularly the *N*-acyl derivatives.[3] In addition to ethano bridge flexing and ring inversion, a third process that involves rotation about the N–CO bond also occurs. In the *N*-acyl derivatives, interaction of the ortho hydrogens inhibits the rotation of the carbonyl group and slows the inversion process of the seven-membered ring.

This paper reports the synthesis and structural determination of new dibenzosilepins (1, X = SiR_2) that contain methyl substituents ortho to the silicon center. At ambient temperature (295 K), 5,5′-bis(trimethylsilyl)-4,6-dimethyl-10,11-dihydro-5*H*-dibenzo[*b*,*f*]silepin (**2**) exhibits a unique conformational rigidity in solution on the NMR time scale without the complications incurred by acyl substitution. The result observed for **2** differs from that for the related silepins 5,5′-bis(trimethylsilyl)-10,11-dihydro-5*H*-dibenzo[*b*,*f*]silepin (**3**) and 4,5,5′,6-tetramethyl-10,11-dihydro-5*H*-dibenzo[*b*,*f*]silepin (**4**), both of which are fluxional down to 183 K.

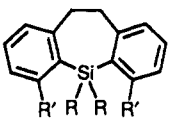

2: R = $Si(Me)_3$; R′ = Me
3: R = $Si(Me)_3$; R′ = H
4: R = Me; R′ = Me

Experimental Section

General Methods. All reactions unless otherwise noted were carried out under an atmosphere of dry nitrogen or argon by using standard Schlenk techniques. Solvents were dried by standard methods and all glassware was dried in an oven at 110–120 °C prior to use. Commercial 2-bromo-*m*-xylene was used as supplied and *N*-bromosuccinimide, NBS, was freshly recrystallized from water before use. The *o*,*o*′-dibromobibenzyl[4] and 2,2-dichloro-1,1,1,3,3,3-hexamethyltrisilane[5] were prepared according to literature methods.

^1H (300 MHz), ^{13}C (75 MHz), and ^{29}Si (59 MHz) NMR spectra were recorded on a Varian XL-300 multinuclear FT NMR spectrometer. For ^1H and ^{13}C, the characteristic solvent peaks were used as internal references. The ^{29}Si spectra are reported with tetramethylsilane as an external standard. $Cr(acac)_3$ was added to **2** and **3** as a relaxation agent for acquiring the silicon data. Fully decoupled ^{13}C and ^{29}Si data are reported. Kugelrohr distillation was employed in all vacuum distillations.

Analyses were performed by Galbraith Laboratories, Inc., Knoxville, TN.

2,2′-Dibromo-3,3′-dimethylbibenzyl. A slurry of 2-bromo-*m*-xylene (19.71 g, 0.173 mol) and NBS (25.32 g, 0.142 mol) in CCl_4 (60 mL) was heated at reflux overnight. After removal of the succinimide (14.08 g, 100%) solvent was removed from the filtrate and the residue distilled. The forerun, bp 54–98 °C (3.0 mmHg) (11.8 g), contained primarily starting material, and the fraction with bp 98–104 °C (3.0 mmHg) (27.17 g) was the desired 2-bromo-3-methylbenzyl bromide (95% from GC analysis). ^1H NMR ($CDCl_3$) δ 2.4 (s, 3 H), 4.6 (s, 2 H), 7.2–7.3 (m, 3 H).

To the benzyl bromide dissolved in ether (100 mL) was added dropwise a solution of phenyllithium in ether (117 mL, 0.44 M). The solution was stirred overnight and then hydrolyzed with a saturated aqueous ammonium chloride solution. The fraction with bp 120–150 °C (0.01 mmHg) contained the bibenzyl, which slowly crystallized (11.64 g, 45% based on starting NBS). Recrystallization from ethanol provided clear crystals, mp 117–118 °C. ^1H NMR ($CDCl_3$) δ 2.4 (s, 6 H), 3.2 (s, 3.7 H), 7.2 (6.2 H). MS, *m*/*e* 366 (based on ^{79}Br). Anal. Calcd for $C_{16}H_{16}Br_2$: C, 52.85; H, 4.32. Found: C, 52.55; H, 4.50.

5,5′-Bis(trimethylsilyl)-4,6-dimethyl-10,11-dihydro-5*H*-dibenzo[*b*,*f*]silepin (2). To a solution of the bibenzyl dibromide (6.0 g, 0.16 mol) in diethyl ether (50 mL) that had been cooled in an ice bath was added *n*BuLi (30 mL, 1.20 M). The mixture was stirred for 1 h before it was cannulated into a pressure addition funnel. A second addition funnel was charged with $Cl_2Si(SiMe_3)_2$ (3.93 g, 0.16 mol) in the same volume of ether, and the two solutions were added simultaneously to ether (50 mL). After it was stirred overnight, the solution was hydrolyzed with saturated aqueous ammonium chloride and the organic layer dried over anhydrous magnesium sulfate. The oil that remained after removal of the volatiles was distilled to give the impure silepin as a viscous liquid, bp 130–160 °C (0.01 mmHg) (2.71 g). Addition of absolute ethanol (2 mL) provided a solid sample of the silepin (0.48 g, mp 102–104 °C). The residue obtained from the ethanol filtrate was purified by elution over silica gel (30 g) with hexanes to provide additional silepin (0.88 g, combined yield, 22%). Two recrystallizations provided an analytical sample of **2**, mp 104.5–105.5 °C. ^1H NMR ($CDCl_3$) δ −0.01 (s, 18 H), 2.4 (s, 6 H), 2.8–3.1 (m, 4 H), 6.9–7.1 (m, 6 H). ^{13}C NMR ($CDCl_3$) δ 1.1, 24.8, 40.6, 125.6, 127.2, 127.6, 136.3, 143.8, 151.9. ^{29}Si NMR ($CDCl_3$) δ −10.45, −41.7. MS, *m*/*e* 382 (M^+), 309 ($M^+ - SiMe_3$). Anal. Calcd for $C_{22}H_{34}Si_3$: C, 69.03; H, 8.95. Found: C, 69.11; H, 9.07.

5,5′-Bis(trimethylsilyl)-10,11-dihydro-5*H*-dibenzo[*b*,*f*]silepin (3). To a solution of *o*,*o*′-dibromobibenzyl (12.6 g, 0.0367 mol) in ether (140 mL), which was cooled in a dry ice/acetone bath, was added *n*BuLi (50 mL, 1.47 M) dropwise over 40 min. After completion of the addition, the cold bath was removed and the solution stirred for 4 h before the resultant slurry was cannulated into a pressure addition funnel. Into a second funnel was placed a solution of $Cl_2Si(SiMe_3)_2$ (6.0 g, 0.024 mol) in ether (100 mL) and the two solutions were added together over a period of 1.2 h. After 10 h at room temperature, the reaction mixture was hydrolyzed with saturated aqueous ammonium chloride solution. The ether layer was dried over anhydrous magnesium sulfate and the volatiles were removed to give a clear, light yellow oil. Distillation provided **3**, bp 127–135 °C (0.01 mmHg) (5.84 g, 68%), which solidified. Two recrystallizations from absolute ethanol provided clear, colorless crystals, mp 87–88 °C. ^1H NMR ($CDCl_3$) δ 0.11 (s, 18 H), 3.0 (s, 4 H), 7.0–7.4 (m, 8 H). ^{13}C NMR ($CDCl_3$) δ 0.20, 39.4, 124.3, 127.5, 128.7, 134.6, 135.9, 151.9. ^{29}Si NMR ($CDCl_3$) δ −14.4, −43.0. MS, *m*/*e* 354 (M^+). Anal. Calcd for $C_{20}H_{30}Si_3$: C, 67.72; H, 8.52. Found: C, 67.20; H, 8.49.

4,5,5′,6-Tetramethyl-10,11-dihydro-5*H*-dibenzo[*b*,*f*]silepin (4). To a solution of dibromide (2.0 g, 5.4 mmol) in ether (25 mL) that had been cooled in an ice bath was added *n*BuLi (9.2 mL, 1.25 M). After the mixture was stirred for about 30 min, the ice bath was removed and the slurry stirred an additional hour. A solution of Me_2SiCl_2 (0.70 g, 5.4 mmol) in ether (25 mL) was added dropwise and the reaction mixture was stirred overnight. After the usual workup, an oily residue was obtained. Distillation provided a fraction with bp 115–135 °C (0.15 mmHg) (0.46 g) as a semisolid. Two recrystallizations from ethanol provided clear crystals of **4**, mp 93–96.5 °C (0.11 g, 8% yield, 95% from GC analysis). ^1H NMR ($CDCl_3$) δ 0.71 (s, 6 H), 2.5 (s, 6 H), 3.1 (s, 4 H), 6.9–7.2 (m, 6 H). ^{13}C NMR ($CDCl_3$) δ 3.6, 24.1, 40.2, 125.6, 128.5, 128.8, 138.3, 144.3, 150.9. ^{29}Si NMR ($CDCl_3$) δ −7.3. MS, *m*/*e* 266 (M^+).

Collection of ^1H NMR Data. All ^1H NMR spectra were recorded on a Varian XL-300 multinuclear spectrometer (300 MHz). Toluene-d_8, chloroform-d_1, and methylene-d_2 chloride were used as received and the residual protons of the deuterated solvents were used as internal standards. Sample concentrations were 30 mg/mL of solvent used in 5-mm (o.d.) XR-55 tubes.

Crystallographic Analysis. Crystal data, data collection, and solution and refinement for **2** and **3** are summarized in Table I. The X-ray studies were carried out on a Siemens R3m/V diffractometer equipped with a highly oriented graphite crystal monochromator. Intensity data were obtained by using Mo Kα radiation (λ = 0.710 69 Å) and were collected by the θ–2θ scan method at variable speed, dependent on peak intensity. Intensities of three standard reflections were monitored after every 50 reflections. Background measurement was 50% of the scan time. Data reduction, structure solution, and refinement of the structures were were carried out by using a Siemens SHELXTL PLUS (VMS) package.[6] No absorption correction was applied to the

(3) (a) Abraham, R. J.; Kricka, L. J.; Ledwith, A. *J. Chem. Soc., Perkin Trans. 2* **1974**, 1648. (b) Ellefson, C. R.; Swenton, L.; Bible, R. H., Jr.; Green, P. M. *Tetrahedron* **1976**, *32*, 1081–1084. (c) Bellucci, G.; Bianchini, R.; Chiappe, C.; Marioni, F. *Tetrahedron* **1988**, *44*, 4863–4870.
(4) Letsinger, R. L.; Skoog, I. H. *J. Am. Chem. Soc.* **1955**, *77*, 5176.
(5) Gilman, H.; Harrell, R. L. *J. Organomet. Chem.* **1966**, *5*, 199.

Table I. Summary of Crystallographic Data for $C_{22}H_{34}Si_3$ (2) and $C_{20}H_{30}Si_3$ (3)

	2	3
molec wt	382.8	354.7
color, habit	colorless, irreg	colorless, needle
cryst size	0.5 × 0.4 × 0.3	0.5 × 0.15 × 0.15
cryst syst	orthorhombic	monoclinic
space group	*Pccn*	*C2/c*
a, *b*, *c*, Å	14.89 (1), 15.98 (2), 20.12 (3)	15.606 (5), 16.061 (5), 8.896 (3)
β, deg	90	102.26 (2)
cell vol, Å^3	4786 (9)	2178.9 (12)
Z	8	4
D(calc), g/cm^3	1.062	1.081
abs coeff, mm^{-1}	0.196	0.210
temp, °C	20	20
scan speed, deg/min in ω	variable, 4.0–15.0	variable, 1.50–15.0
scan range (ω)	0.80° + Kα sep	0.60° + Kα sep
2θ range, deg	3.5–45.0	3.5–45.0
index ranges	$0 < h < 16$, $0 < k < 17$, $0 < l < 21$	$-16 < h < 16$, $0 < k < 17$, $0 < l < 9$
unique data	3117	1439
obsd data	719	617
R	5.40%	5.53%
R_w	6.38%	5.86%
weighting scheme	$w^{-1} = \sigma^2(F) + 0.001F^2$	unit wt
largest, mean Δ/σ	0.022, 0.001	0.004, 0.0
goodness of fit	1.21	2.57
lgst diff peak, e Å^{-3}	0.29	0.34
lgst diff hole, e Å^{-3}	0.25	0.29

Table II. Atomic Coordinates (×10^4) and Equivalent Isotropic Displacement Coefficients (Å^2 × 10^3) for 2[a]

	x	*y*	*z*	*U*(eq)[b]
Si(1)	2500	7500	4907 (3)	51 (3)
Si(2)	2500	2500	2607 (3)	42 (2)
Si(3)	3578 (3)	3364 (3)	3155 (2)	62 (2)
Si(4)	1208 (3)	8043 (3)	4352 (2)	63 (2)
C(11)	1973 (8)	6602 (8)	5404 (7)	47 (4)
C(12)	1790 (9)	6637 (9)	6103 (8)	70 (5)
C(13)	1368 (9)	5967 (10)	6393 (8)	93 (6)
C(14)	1112 (9)	5288 (10)	6043 (9)	89 (6)
C(15)	1245 (9)	5225 (9)	5389 (8)	79 (5)
C(16)	1694 (9)	5891 (9)	5055 (7)	63 (5)
C(17)	1779 (8)	5789 (8)	4318 (7)	89 (6)
C(18)	2007 (7)	7402 (10)	6491 (6)	97 (6)
C(41)	1331 (8)	8146 (8)	3428 (6)	89 (5)
C(42)	933 (9)	9077 (8)	4727 (7)	98 (6)
C(43)	212 (8)	7370 (8)	4512 (7)	99 (6)
C(21)	1873 (8)	3339 (7)	2123 (7)	41 (4)
C(22)	2012 (9)	3509 (9)	1455 (7)	57 (4)
C(23)	1596 (9)	4201 (9)	1128 (7)	74 (5)
C(24)	1056 (10)	4690 (10)	1509 (8)	88 (6)
C(25)	898 (9)	4564 (8)	2142 (8)	70 (5)
C(26)	1297 (8)	3867 (9)	2484 (7)	52 (4)
C(27)	1138 (8)	3807 (8)	3207 (6)	72 (5)
C(28)	2622 (9)	2972 (6)	1027 (6)	64 (5)
C(31)	3608 (10)	3274 (9)	4072 (7)	139 (7)
C(32)	3353 (8)	4488 (7)	2952 (7)	73 (5)
C(33)	4691 (8)	3144 (8)	2780 (7)	110 (6)

[a] Two half-molecules per asymmetric unit. [b] Equivalent isotropic *U* defined as one-third of the trace of the orthogonalized U_{ij} tensor.

data. The structures were solved by direct methods and refined by full-matrix least squares by minimizing the $\sum w(F_o - F_c)^2$. Due to lack of observed data ($F > 6.0\sigma(F)$), only Si atoms were refined anisotropically. All non-hydrogen atoms were refined isotropically to convergence. Hydrogen atoms were included in their calculated positions and were refined by using a riding model and fixed isotropic temperature factors.

(6) Sheldrick, G. M. Siemens Analytical X-ray Division, Madison, WI, 1989.

Table III. Bond Distance (Å) and Bond Angles (deg) for 2[a]

Bond Distances			
Si(1)–Si(4)	2.388 (6)	Si(1)–C(11)	1.92 (1)
Si(1)–Si(4A)	2.388 (6)	Si(1)–C(11A)	1.92 (1)
Si(2)–Si(3)	2.386 (6)	Si(2)–C(21)	1.90 (1)
Si(2)–Si(3A)	2.386 (6)	Si(2)–C921A)	1.90 (1)
Si(3)–C(31)	1.85 (2)	Si(3)–C(32)	1.87 (1)
Si(3)–C(33)	1.86 (1)	Si(4)–C(41)	1.88 (1)
Si(4)–C(42)	1.86 (1)	Si(4)–C(43)	1.86 (1)
C(11)–C(12)	1.43 (2)	C(11)–C(16)	1.40 (2)
C(12)–C(13)	1.37 (2)	C(12)–C(18)	1.49 (2)
C(13)–C(14)	1.35 (2)	C(14)–C(15)	1.34 (2)
C(15)–C(16)	1.42 (2)	C(16)–C(17)	1.50 (2)
C(18)–C(18A)	1.50 (2)	C(21)–C(22)	1.39 (2)
C(21)–C(26)	1.41 (2)	C(22)–C(23)	1.43 (2)
C(22)–C(28)	1.52 (2)	C(23)–C(24)	1.36 (2)
C(24)–C(25)	1.31 (2)	C(25)–C(26)	1.44 (2)
C(26)–C(27)	1.48 (2)	C(28)–C(28A)	1.55 (2)
Bond Angles			
Si(4)–Si(1)–C(11)	100.7 (4)	Si(4)–Si(1)–Si(4A)	124.2 (3)
C(11)–Si(1)–Si(4A)	107.6 (4)	Si(4)–Si(1)–C(11A)	107.6 (4)
C(11)–Si(1)–C(11A)	117.2 (9)	Si(4A)–Si(1)–C(11A)	100.7 (4)
Si(3)–Si(2)–C(21)	99.2 (4)	Si(3)–Si(2)–Si(3A)	125.0 (3)
C(21)–Si(2)–Si(3A)	108.3 (4)	Si(3)–Si(2)–C(21A)	108.3 (4)
C(21)–Si(2)–C(21A)	118.3 (9)	Si(3A)–Si(2)–C(21A)	99.2 (4)
Si(2)–Si(3)–C(31)	115.6 (5)	Si(2)–Si(3)–C(32)	109.5 (4)
C(31)–Si(3)–C(32)	107.2 (6)	Si(2)–Si(3)–C(33)	107.7 (5)
C(31)–Si(3)–C(33)	111.6 (7)	C(32)–Si(3)–C(33)	104.6 (6)
Si(1)–Si(4)–C(41)	114.6 (4)	Si(1)–Si(4)–C(42)	108.1 (5)
C(41)–Si(4)–C(42)	110.2 (6)	Si(1)–Si(4)–C(43)	110.6 (4)
C(41)–Si(4)–C(43)	107.5 (6)	C(42)–Si(4)–C(43)	105.5 (6)
Si(1)–C(11)–C(12)	124.0 (1)	Si(1)–C(11)–C(16)	118.0 (1)
C(12)–C(11)–C(16)	118.0 (1)	C(11)–C(12)–C(13)	118.0 (1)
C(11)–C(12)–C(18)	120.0 (1)	C(13)–C(12)–C(18)	121.0 (1)
C(12)–C(13)–C(14)	122.0 (2)	C(13)–C(14)–C(15)	122.0 (2)
C(14)–C(15)–C(16)	119.0 (1)	C(11)–C(16)–C(15)	120.0 (1)
C(11)–C(16)–C(17)	124.0 (1)	C(15)–C(16)–C(17)	115.0 (1)
C(12)–C(18)–C(18A)	113.0 (1)	Si(2)–C(21)–C(22)	124.0 (1)
Si(2)–C(21)–C(26)	117.0 (1)	C(22)–C(21)–C(26)	118.0 (1)
C(21)–C(22)–C(23)	122.0 (1)	C(21)–C(22)–C(28)	112.0 (1)
C(23)–C(22)–C(28)	116.0 (1)	C(22)–C(23)–C(24)	116.0 (1)
C(23)–C(24)–C(25)	125.0 (2)	C(24)–C(25)–C(26)	121.0 (1)
C(21)–C(26)–C(25)	118.0 (1)	C(21)–C(26)–C(27)	125.0 (1)
C(25)–C(26)–C(27)	117.0 (1)	C(22)–C(28)–C(28A)	114.0 (1)

[a] Two half-molecules per asymmetric unit. See Figure 3 for numbering correlations.

Table IV. Atomic Coordinates (×10^4) and Equivalent Isotropic Displacement Coefficients (Å^2 × 10^3) for 3

	x	*y*	*z*	*U*(eq)[a]
Si(1)	0	2922 (2)	2500	49 (1)
Si(2)	−646 (2)	2107 (2)	362 (3)	62 (1)
C(1)	927 (5)	3560 (5)	2002 (9)	42 (2)
C(2)	1508 (5)	3138 (6)	1275 (10)	68 (3)
C(3)	2247 (6)	3516 (6)	939 (11)	75 (3)
C(4)	2407 (6)	4338 (5)	1318 (9)	64 (3)
C(5)	1844 (5)	4770 (5)	2014 (9)	57 (2)
C(6)	1097 (5)	4404 (5)	2338 (9)	45 (2)
C(7)	464 (4)	4917 (5)	3010 (9)	55 (2)
C(8)	88 (6)	1280 (6)	−127 (12)	94 (3)
C(9)	−1638 (6)	1581 (6)	740 (11)	91 (4)
C(10)	−955 (6)	2827 (6)	−1311 (10)	93 (3)

[a] Equivalent isotropic *U* defined as one-third of the trace of the orthogonalized U_{ij} tensor.

A colorless prism obtained from recrystallization of **2** from absolute ethanol was used for X-ray diffraction. The compound crystallizes in the space group *Pccn*. Refinement of positional and isotropic thermal parameters of all non-hydrogen atoms followed by anisotropic refinement of silicon led to final *R* values of $R = 0.054$ and $R_w = 0.064$. Atomic coordinates and equivalent isotropic displacement coefficients for compound **2** are given in Table II. Bond distances and angles for **2** are listed in Table III.

Colorless needles of **3** for X-ray diffraction were obtained by recrystallization from absolute ethanol. The structure was solved

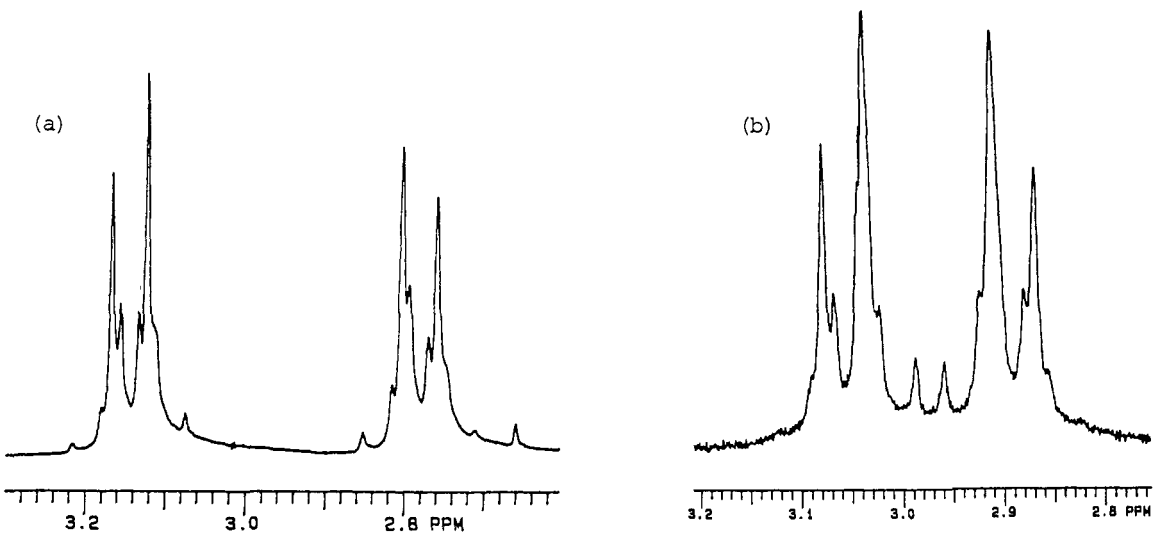

Figure 1. Ethano bridge region of room temperature (291 K) spectra of compound **2** in (a) chloroform-d_1 and (b) toluene-d_8.

Table V. Bond Distances (Å) and Bond Angles (deg) for 3

	(a) Bond Distances		
Si(1)-Si(2)	2.352 (3)	Si(1)-C(1)	1.900 (8)
Si(1)-Si(2A)	2.352 (3)	Si(1)-C(1A)	1.900 (8)
Si(2)-C(8)	1.86 (1)	Si(2)-C(9)	1.86 (1)
Si(2)-C(10)	1.87 (1)	C(1)-C(2)	1.40 (1)
C(1)-C(6)	1.40 (1)	C(2)-C(3)	1.39 (1)
C(3)-C(4)	1.37 (1)	C(4)-C(5)	1.37 (1)
C(5)-C(6)	1.39 (1)	C(6)-C(7)	1.50 (1)
C(7)-C(7A)	1.54 (1)		
	(b) Bond Angles		
Si(2)-Si(1)-C(1)	109.2 (2)	Si(2)-Si(1)-Si(2A)	112.4 (2)
C(1)-Si(1)-Si(2A)	105.8 (2)	Si(2)-Si(1)-C(1A)	105.8 (2)
C(1)-Si(1)-C(1A)	114.8 (5)	Si(2A)-Si(1)-C(1A)	109.2 (2)
Si(1)-Si(2)-C(8)	114.0 (3)	Si(1)-Si(2)-C(9)	109.7 (3)
C(8)-Si(2)-C(9)	107.1 (5)	Si(1)-Si(2)-C(10)	107.1 (3)
C(8)-Si(2)-C(10)	108.9 (5)	C(9)-Si(2)-C(10)	110.0 (4)
Si(1)-C(1)-C(2)	116.6 (6)	Si(1)-C(1)-C(6)	126.2 (6)
C(2)-C(1)-C(6)	117.1 (7)	C(1)-C(2)-C(3)	122.5 (8)
C92)-C(3)-C(4)	118.9 (9)	C(3)-C(4)-C(5)	119.9 (9)
C(4)-C(5)-C(6)	121.8 (8)	C(1)-C(6)-C(5)	119.7 (7)
C(1)-C(6)-C(7)	120.2 (7)	C(5)-C(6)-C(7)	120.1 (7)
C(6)-C(7)-C(7A)	112.4 (7)		

by direct methods and successfully refined in the space group $C2/c$. Full-matrix refinement led to convergence at values of R = 0.055 and R_w = 0.059. Atomic coordinates and equivalent isotropic displacement coefficients for compound **3** are given in Table IV. Bond distances and angles for **3** are given in Table V.

Results

Interpretation of NMR Data. The singlet for the ethano bridge hydrogens observed at δ 3.01 and δ 3.09, for **3** and **4**, respectively (A_4), indicate that these two silepins undergo rapid ring inversion on the NMR time scale at ambient probe temperatures. In contrast, under similar conditions, **2** exhibits an AA'BB' pattern for the ethano bridge protons at δ 2.76–3.13 in chloroform-d_1 and δ 2.85–3.10 in toluene-d_8 (Figure 1). The resonances for **2** coalesce with increasing temperatures to an A_4 system (T_c = 353 K). A HETCOR spectrum revealed chemically nonequivalent protons on each ethano bridge carbon. The ^{13}C NMR spectrum for **2** has three aliphatic (Me_3Si, CH_2CH_2, and Me) and six aromatic resonances and the ^{29}Si NMR spectrum exhibits two resonances for the two types of silicon atoms.

Variable-temperature spectra were obtained in both chloroform-d_1 up to 313 K and toluene-d_8 up to 358 K. The chemical shift difference in chloroform at 291 K is large emough (109 Hz) to be evaluated as an AA'XX' spin system. This spectrum was used to assign lines and to calculate coupling constants: $J_{AB(A'B')}$ = −12.5, $J_{AB'(A'B)}$ = 0.7, $J_{AA'}$ = 6.8, $J_{BB'}$ = 0.4 Hz. The assignment of lines, coupling constants, and their signs was tested and confirmed using RACOON.[7] The dynamic process was analyzed by spin simulation using DNMR4 for the four spin, two configuration case.[8] The relaxation time (T_2*) was estimated from line-width measurements evaluated at half-height from the spectrum obtained at 291 K. The populations of the two conformations were entered as 50–50 over the range of temperatures since the protons are diastereotopic due to the symmetry of the molecule. The rate constant (k) was varied and a set of theoretical band shapes was generated. These bandshapes could be matched with the actual spectra obtained at varying tempertures as shown in Figure 2. The free energy of activation (ΔG^*) was calculated to be 16 kcal/mol from the coalescence data.

Solid-State Conformation. Compound **2** crystallizes with two crystallographically distinct molecules, half of each being unique, and the halves are related by a crystallographic 2-fold axis of symmetry as shown by the numbering of **2A** and **2B** (only the unique atoms are labeled) in Figure 3.[9] The nonplanar tricyclic framework exhibits bend angles[10] of 160 and 153°. A view along the C(10)-C(11) axis of the ethano bridge with the dihedral angles obtained from the solid-state data is shown in Figure 4a and shows a nearly eclipsed conformation.

A projection view and atom numbering for **3** is shown in Figure 5. This molecule also exhibits crystallographic C_2 symmetry, hence only half of the molecule is unique. The framework of **3** is slightly more folded with a bend

(7) Really Awesome Computer Calculation of Observed NMR Spectra. Version 2.0, Schatz, P. F., Department of Chemistry, University of Wisconsin—Madison, Madison, WI. Distributed by "Project Seraphim", supported by NSF Development in Science Education, J. W. Moore, Director, Department of Chemistry, Eastern Michigan University, Ypsilanti, MI.

(8) DNMR4: Calculation of Chemically Exchanging Spectra. Bushweller, C. H.; Letenore, L. J.; Brunelle, J. A.; Bilofsky, H. S.; Whalon, M. R.; Fleischman, S. H.; Department of Chemistry, University of Vermont, Burlington, VT. Distributed by Quantum Chemistry Program Exchange, Department of Chemistry, Indiana University, Bloomington, IN.

(9) The ethano bridge carbons are labeled C(18,18a) and C(28,28a) in the solid-state structures and C(10), C(11) in IUPAC nomenclature. For convenience and clarity, reference to specific atoms will use IUPAC numbering.

(10) (a) Wilhelm, M.; Kuhn, R. *Pharmakopsychiatr. Neuro-Psychopharmakol.* **1970**, *3*, 317–332. (b) Wilhelm, M. *Pharm. J.* **1975**, *214*, 414–416.

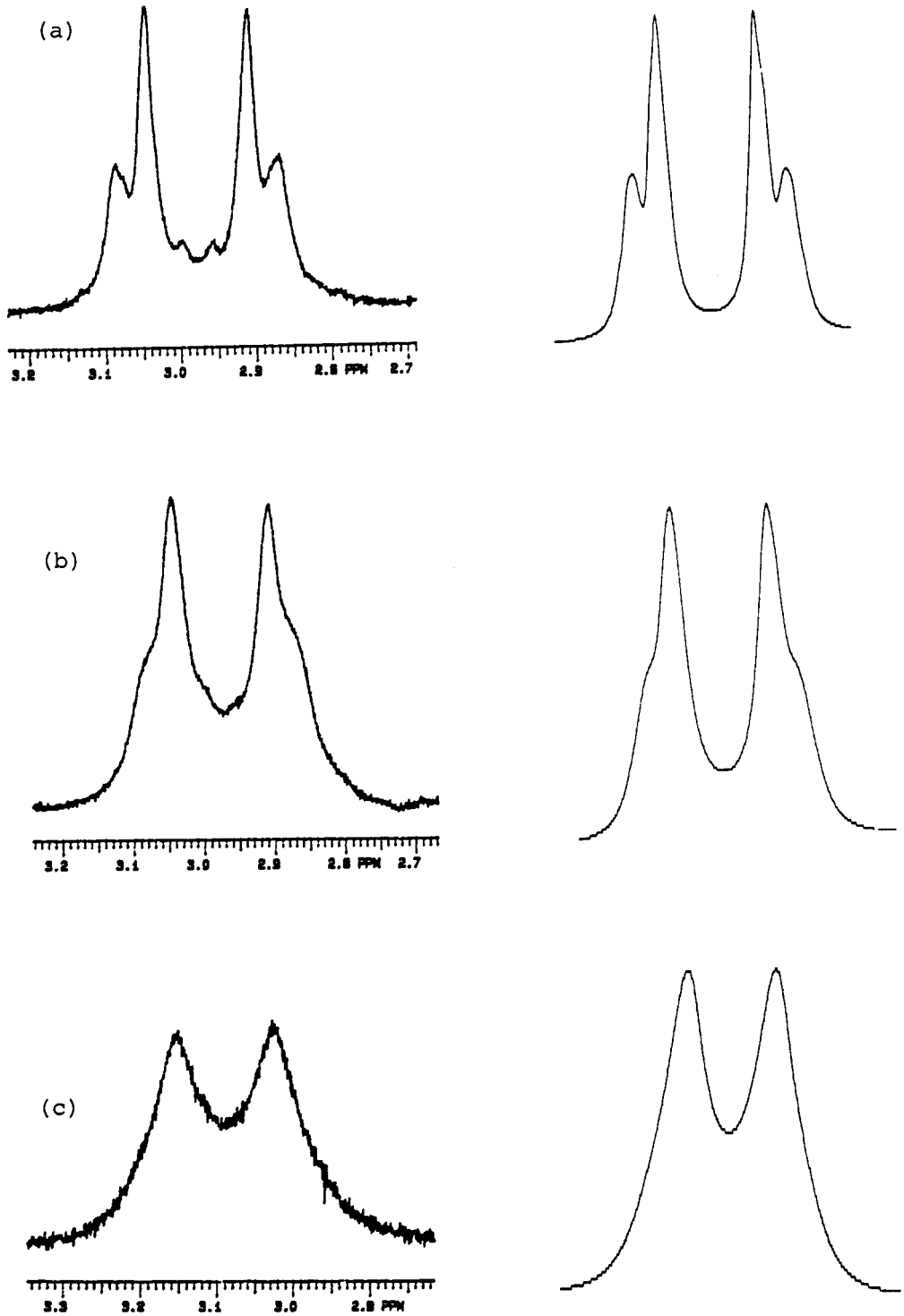

Figure 2. Observed and calculated spectra for the ethano bridge region of compound **2** in toluene-d_8 at (a) 45, (b) 55, and (c) 65 °C.

angle of 149°. A view along the C(10)–C(11) axis of the ethano bridge with the dihedral angles obtained from the solid state is shown in Figure 4b.

Discussion

The structures of several dibenzoheteroepin systems have been determined in the solid state, but few systems can be analyzed in solution by NMR methods since the framework is flexible and the ethano bridge protons normally appear as a singlet.[1b] The observation of this singlet implies rapid ring inversion. Notable exceptions are 5-acyliminobibenzyls (1, X = NC(O)R),[3a] a dihydrodibenzo[*b*,*f*]phosphepin (1, X = P(O)Cl),[11] and oxepins (1, X = O) substituted in the 10-position.[12] Recently, the solid-state structures of the mono tricarbonylchromium complexes of 1 (X = CH_2, CHOH, and C=O) have been determined and, although these systems are highly flexible, the conformational properties were analyzed with the use of a lanthanide-induced shift method.[13]

(11) Segall, Y.; Shirin, E.; Granoth, I. *Phosphorus Sulfur* **1980**, *8*, 243.
(12) Kametani, T.; Shibuya, S.; Ollis, W. D. *J. Chem. Soc. C* **1968**, *23*, 2877.
(13) Weissensteiner, W.; Hofer, O.; Wagner, U. G. *J. Org. Chem.* **1988**, *53*, 3988.

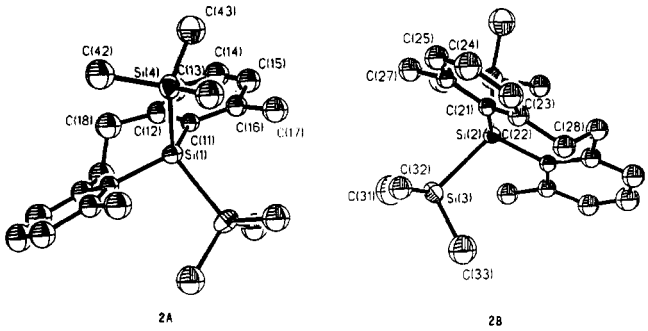

Figure 3. Projection view of compound **2**. Thermal ellipsoids are drawn to 30% probability. Hydrogen atoms are omitted for clarity.

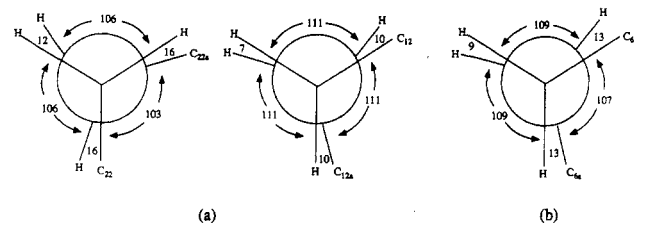

Figure 4. View down the ethano bridge as calculated from the solid-state data for (a) compound **2** and (b) compound **3**. (Hydrogens are shown in calculated positions.)

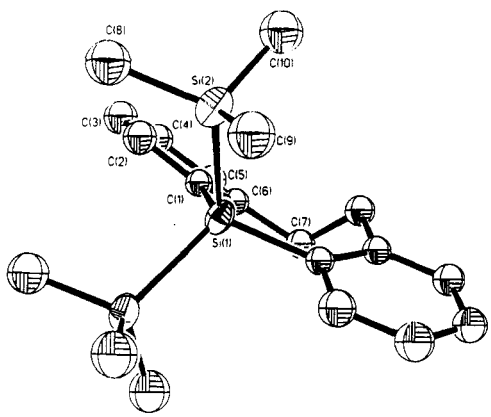

Figure 5. Projection view of compound **3**. Thermal ellipsoids are drawn to 30% probability. Hydrogen atoms are omitted for clarity.

Examination of the coupling constants and the HETCOR spectrum shows that each ethano bridge carbon of **2** has chemically nonequivalent hydrogens and an analysis of the coupling constants is consistent with a trans orientation of the equivalent hydrogens. This observation is in contrast to that observed in the azepine systems (1, X = NC(O)R), where the equivalent hydrogens are assigned a cis orientation. The published room temperature spectrum of **5**[3a] is more complex than that shown for **2** in Figure

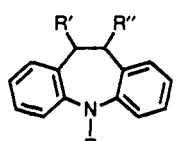

5: R = $COCH_3$; R' = R'' = H
6: R = $COCH_2Cl$; R' = R'' = H
7: R = CO_2Et; R' = R'' = H
8: R = COCl; R' = Br; R'' = OH

1. The trans coupling constant for **2** is lower than that in the only two systems for which comparable measurements

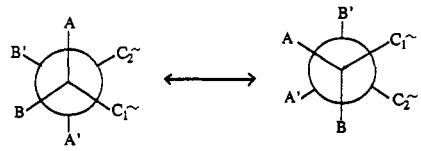

Figure 6. Proposed ethano bridge flexing for compound **2**.

have been made (1, X = NC(O)R and P(O)Cl) but falls within the range 6.0–8.5 Hz reported for a series of 10-substituted oxepins (1, X = O).[12]

The AA'BB' pattern exhibited by the ethano bridge of **2** as shown in Figure 1 suggests that some process occurs for this system that is slow on the NMR time scale. The low-temperature limit, when the molecule is completely rigid, would be expected to exhibit a complex ABCD spin system rather than the simpler AA'BB' system. The broadness of lines in the observed room temperature spectrum indicates that the low-temperature limit has not been reached and the ethano bridge resonances remain unchanged down to 183 K. Since the room temperature ^{13}C NMR spectrum shows only six aromatic and three aliphatic resonances with no sign of line broadening, a process that makes the two halves of the molecule equivalent on the NMR time scale must be occurring. Thus, the spectrum obtained at room temperature for **2** is a consequence of ethano bridge flexing as illustrated in Figure 6. Equation 1, derived from the Karplus correlation,[14] where R is the ratio of J_{trans} to J_{cis}, if $J_{AB'}$ is cis and $J_{AA'}$ is trans, allows for calculation of the $C_{ar}CH_2CH_2C_{ar}$ dihedral angle for the ethano bridge in solution. Flexing of the ethano bridge for all three silepins is observed in solution down to 183 K and must be the lowest energy process.

$$\cos \phi = [3/(2 + 4R)]^{1/2} \quad (1)$$

Table VI summarizes data for the $C_{ar}CH_2CH_2C_{ar}$ dihe-

(14) Garbisch, E. W.; Griffith, M. C. *J. Am. Chem. Soc.* **1968**, *90*, 6543.
(15) IBMNEWST. Copyright by B.O. Loopstra, Laboratory for Crystallography, University of Amsterdam, Nieuwe Actergracht 166, 1018 W V Amsterdam, The Netherlands.
(16) Reboul, J. P.; Cristau, B.; Pepe, G. *Acta Crystallogr.* **1981**, *B37*, 394.
(17) Reboul, J. P.; Soyfer, J. C.; Cristau, B.; Caranoni, C.; Pepe, G. *Acta Crystallogr.* **1982**, *B38*, 2633.
(18) Wagner, A. *Acta Crystallogr.* **1980**, *B36*, 813.
(19) Larsson, K. *Acta Chem. Scand.* **1970**, *24*, 1503.
(20) Tokuma, Y.; Nojima, H.; Morimoto, Y. *Bull. Chem. Soc. Jpn.* **1971**, *44*, 2665.
(21) Tokuma, Y.; Koda, S.; Tsubouchi, S.; Morimoto, Y. *Bull. Chem. Soc. Jpn.* **1971**, *44*, 2665.
(22) Reboul, J. P.; Soyfer, J. C.; Cristau, B.; Darbon, N.; Oddon, Y.; Pepe, G. *Acta Crystallogr., Sect. C: Cryst. Struct. Commun.* **1983**, *C39*, 600.
(23) Herrman, W. A.; Plank, J.; Kriechbaum, G. W.; Ziegler, M. L.; Pfisterer, H.; Atwood, W. A.; Rogers, R. D. *J. Organomet. Chem.* **1984**, *264*, 327.
(24) Bandolini, G.; Nicolini, M. *J. Crystallogr. Spectrosc. Res.* **1983**, *13*, 191.
(25) Reboul, J. P.; Cristau, B.; Estienne, J.; Astier, J. P. *Acta Crystallogr.* **1980**, *B36*, 2108.
(26) Post, M. L.; Kennard, O.; Horn, A. S. *Acta Crystallogr.* **1975**, *B31*, 1008.
(27) Paulus, V. E. F. *Acta Crystallogr.* **1978**, *B34*, 1942.
(28) Post, M. L.; Horn, A. S. *Acta Crystallogr.* **1977**, *B33*, 2590.
(29) Hallberg, A.; Hintermeister, N. M.; Martin, A. R.; Bates, R. B.; Ortega, R. B. *Acta Crystallogr.* **1984**, *C40*, 2110.
(30) Ueda, I.; Tashiro, C. *Acta Crystallogr.* **1984**, *C40*, 422.
(31) Allen, D. W.; Nowell, I. W.; Walker, P. E. *Z. Naturforsch. Teil* **1980**, *B35*, 133.
(32) Cynkier, I.; Furmanova, N. *Cryst. Struct. Commun.* **1980**, *9*, 307.
(33) Corey, E. R.; Corey, J. Y.; Glick, M. D. *J. Organomet. Chem.* **1977**, *129*, 17.
(34) Paton, W. F.; Cody, V.; Corey, E. R.; Corey, J. Y.; Glick, M. D. *Acta Crystallogr.* **1976**, *B32*, 2509.

Table VI. $C_{ar}CH_2CH_2C_{ar}$ Dihedral Angle Determined from Crystallographic and Solution Data for 10,11-Dibenzo[*b*,*f*]heteroepins

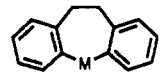

M	solid[a] range	solid[a] av (no. struct)	M	solution $J_{1,3}$	solution $J_{2,3}$	solution $J_{1,2}$	solution calcd[b] ϕ	ref
CHR[c]	55–72	61.5 (4)	CH_2		(A_4)			
			CH_2[d]	−15.4, −16.2	8.8	4.3	55 (125)[e]	13
			CHOH[d]	−15.5, −16.3	12.2	4.8	52.5 (127.5)[e]	13
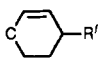	81, 84[g]	82.5						
C=X[h]	58–83	70 (8)	C=O		(A_4)			13
			C=O[d]	−15.0	10.2 (cm)[i]	1.0	74 (106)[e]	13
			$Mn(CO)_2Cp$					
N—R[j]	49–79[k]	62 (11)	NAc	−15.8	8.68	5.09	51 (129)	3a
P(O)Ph[l]	67	67	P(O)Cl	−15.8	7.9	6.0	47 (133)	11
BOR[m]	88, 92	90						
SiRR'[n]	88–92	90 (4)			(A_4)			*n*
$Si(SiMe_3)_2$	107	107			(A_4)			this work
$Si(SiMe_3)_2$[o]	103, 111	107		−12.5	6.8 (0.4)	0.7	74 (106)	this work

[a] Newman projection down the C_{10}–C_{11} bond. Values are published solid-state data or calculated with the IBMNEWST program from published solid-state data.[15] [b] Values calculated by using negative cos ϕ are given in parentheses. [c] R = H;[16] H, $Cr(CO)_3$ complex;[13] N(CH_2)$_6CO_2H$;[17] OH, $Cr(CO)_3$ complex.[13] [d] $Cr(CO)_3$ complex.[13] [e] Calculated from the published data in ref 3 by eq 1. [f] R = NMe_2H^+, 3-chloro substituent.[18] [g] Two molecules in the asymmetric unit.[17] [h] X = CHBr;[19] piroheptine–HBr;[20f] piroheptine–HBr, 2-hydroxy substituent;[21] O;[22] O, $Cr(CO)_3$ complex;[13] $Mn(CO)_2Cp$;[23] $NO(CH_2)_2NHMe_2$·HCl.[24] [i] Not analyzed. [j] R = H;[25] $(CH_2)_3NMe_2$·HCl;[26f] $(CH_2)_3NMe_2$·HBr;[27f] $(CH_2)_3NMe_2$·HCl, 3-chloro substituent;[28] $(CH_2)_3NMe_2$·HCl, 4-chloro substituent.[29] R = $(CH_2)_3NR_2$: NR_2: R_2 = 4-carbamoyl-4-piperidinopiperidino; 2-oxo-1,2,3,4,5,6,7,8,8a-octahydroimidazo(1,2-*a*)pyridine-3-spiro-4′-piperidino, 3-chloro substituent; 2-oxo-1,2,3,5,6,7,8,8a-octahydroimidazo(1,2-*a*)pyridine-3-spiro-4′-piperidino.[30] [k] Lowest value in doubt due to disorder of ethano bridge. [l] Reference 31.[31] [m] Bis(4-dibenzoborepinyl) ether.[32] [n] R = Ph, R′ = Me,[33] OMe;[34] R = *p*-$C_6H_4NMe_2$, R′ = H;[35] R = $(CH_2)_3NMe_2$·HCl, R′ = Me.[36] [o] 4,6-Methyl substituents.

dral angle as determined in the solid state for 1 (X = sp^3 C, sp^2 C, N, P, B, Si), **2** and **3**, as well as values determined from ^1H NMR in solution. The only compounds for which data are available for both solution and the solid state are **2** and the flexible chromium tricarbonyl complexes of 1 (X = CH_2, CHOH, C=O). The dihedral angles calculated from the NMR data for 1 (X = sp^3 C, sp^2 C, NR) are reasonably close to the average solid-state value for the respective class; however, this is not the case for the phosphepin (1, X = P(O)Cl). From eq 1 and the appropriate coupling constants, if the cos ϕ is positive (comparable to the previously reported investigations), the dihedral angle for **2** in solution is calculated to be 74°. Using a negative cos ϕ, the dihedral angle is found to be 106°. The latter value is more closely related to the solid-state average value of 107° for **2**. The value of ϕ for silepins (and the single borepin) in the solid state are significantly larger than for the other compounds listed in Table VI. Both **2** and **3**, with large exocyclic substituents exhibit ϕ values larger than those of previously reported silepins.

Torsion around $C_{ar}SiC_{ar}$ bonds is expected to be lower in energy than in the comparable azepine systems;[37] therefore, both ethano bridge flexing and ring inversion are expected to be low-energy processes compared with the azepine systems. As expected, both **3** and **4** exhibit ring inversion at room temperature in addition to ethano bridge flexing. However, once the ortho hydrogens in **3** are replaced by methyl groups to produce **2**, ring inversion becomes a high-energy process and does not occur at room temperature as supported by the observations that $J_{AA'}$ does not equal $J_{BB'}$. In order for coalescence to occur to an A_4 system, a combination of ethano bridge flexing and ring inversion is required. As the temperature of a solution of **2** is increased, the rate of ethano bridge flexing increases and is eventually accompanied by ring inversion. The value of ΔG^* of 16 kcal/mol is assigned to the ring inversion process for **2** and is in close agreement with those values reported for the *N*-acyliminobibenzyl derivatives (5–7) (ΔG^* = 13.5–20 kcal/mol)[3a] and the value calculated for the bridge-substituted species (8) (ΔG^* = 16.5 kcal/

Table VII. Comparison of Dibenzotricyclic Structural Parameters

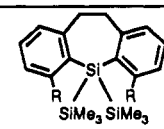

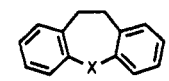

	R = Me[a] (2) A	R = Me[a] (2) B	R = H[b] (3)	X = MeSiR[c]	X = NR[d] A	X = NR[d] B
bend angle, deg	160	153	149	141	130	123
dist btwn benzo centers, Å	5.78	5.79	5.73	5.61	4.96	4.79
skew dist, Å	0.22	0.26	0.29	0.31	0.67	0.61
twist angle, deg	23.2	28.2	28.8	22.9	17.2	8.4

[a] This work. Two crystallographically distinct molecules per asymmetric unit (half of each unique). [b] This work. One-half of the molecule unique. [c] Silipramine, R = $(CH_2)_3N(CH_3)_2$·HCl·H_2O.[36] [d] Imipramine, R = $(CH_2)_3N(CH_3)_2$·HCl. Two molecules per asymmetric unit.[26]

(35) Corey, E. R.; Corey, J. Y.; Glick, M. D. *J. Organomet. Chem.* **1975**, *101*, 177.
(36) Corey, E. R.; Corey, J. Y.; Glick, M. D. *Acta Crystallogr.* **1976**, *B32*, 2025.
(37) For a comprehensive comparison of silicon and carbon, see: Corey, J. Y. In *The Chemistry of Organic Silicon Compounds*; Patai, S., Rappoport, Z., Eds.; John Wiley and Sons: New York, 1989; Part I, pp 1–56.

mol).[3c] The *N*-acyl compounds require the additional process of free rotation about the N-C bond for ring inversion to occur.

A set of parameters has previously been developed to describe the solid-state structural features of dibenzotricyclic systems.[10a,35] The values for these parameters are summarized in Table VII for **2** and **3** and are compared to those of related tricycles, silipramine,[36] and imipramine.[26] The replacement of nitrogen in **1** (X = NR) by the larger silicon center (**1**, X = SiRR') results in flattening of the tricyclic framework as demonstrated by the increase in the bend angles relative to imipramine. The increase in the bend angle is paralleled by an increase in the distance between the benzo group centers. Addition of substituents in positions ortho to the silicon heteroatom flattens the framework further.

The skew distance, the difference between nonbonded benzo carbon distances across the central ring, is primarily a function of the covalent radius of X in **1**.[35] The larger silicon atom provides a spacing closer to that of the ethano bridge and is reflected in the smaller skew distances relative to imipramine. The decreases in the skew distance through the sequence silipramine, **3**, **2** result from a small increase in the endocyclic Si-C bond lengths through this series from 1.870 (4)[35] to 1.92 (1) Å.

The major difference between **2** and **3** in the solid state is an appreciable widening of the Si-Si-Si angle from a value of 112° in **3** to 124° and 125° in the two independent molecules of **2**. The widening of the angle in **2** decreases the interaction of the exocyclic trimethylsilyl groups with ortho methyl substituents. Consistent with this observation are the longer Si-Si bond lengths in **2** relative to **3**. Smaller substituents on the silicon heteroatom should exhibit a decreased interaction with the ortho methyl groups. To test this hypothesis, the silepin related to **2** with exocyclic methyl substituents, **4**, was synthesized and indeed **4** undergoes rapid ring inversion down to 183 K. It is not clear how bulky the organic substituents on silicon must be to conformationally lock the tricylic framework. There is at least one report which demonstrates that a trimethylsilyl substituent behaves as a bulkier group than a *tert*-butyl group.[38] The series of compounds in this study demonstrate that to increase the barrier to ring inversion of a dibenzosilacycle will require the combination of a substituent in positions ortho to the silicon heteroatom and sufficiently bulky exocyclic substituents.

Acknowledgment. The Weldon Spring Fund of the University of Missouri—St. Louis is acknowledged for support of this work. The Hewlett-Packard 5988A GC/MS system was purchased with support of the National Science Foundation (Grant CHE-8813154). We appreciate helpful discussions with C. Maryanoff, B. Maryanoff, R. E. K. Winter, G. Anderson, S. Barcza, and F. Homan. We also appreciate the administrative assistance of R. Schneider and the technical assistance of J. Kramer.

Supplementary Material Available: Tables of anisotropic thermal parameters and hydrogen coordinates and thermal parameters and figures showing stereoviews (4 pages); tables of observed and calculated structure factors (19 pages). Ordering information is given on any current masthead page.

(38) Okazaki, R.; Unno, M.; Inamoto, N. *Chem. Lett.* **1989**, 791.

Triazine Adducts of Dimethylzinc and Dimethylcadmium: X-ray Crystal Structure of $Me_2Zn[(CH_2NMe)_3]_2$

Michael B. Hursthouse,* Majid Motevalli, Paul O'Brien,* and John R. Walsh

Department of Chemistry, Queen Mary and Westfield College, University of London, Mile End Road, London, E1 4NS U.K.

Anthony C. Jones*

Epichem Ltd., Power Road, Bromborough, Wirral, Merseyside, L62 3QF U.K.

Received January 16, 1991

The reaction of various triazines of the type $(CH_2NR)_3$ with dimethylzinc and dimethylcadmium yielded a series of adducts of the type $Me_2M[(CH_2NR)_3]_2$ (where M = zinc or cadmium and R = methyl, ethyl, or isopropyl), of which the methyl derivative of dimethylzinc has proved useful in the growth of high-quality ZnSe by metalloorganic vapor deposition (MOCVD). The X-ray crystal structure of $Me_2Zn[(CH_2NMe)_3]_2$ has been determined and shows the complex to consist of monomeric units of C_{2v} symmetry. The compound crystallizes in space group *Cmcm*, a = 13.553 (2) Å, b = 7.399 (2) Å, and c = 19.738 (4) Å, $\alpha = \beta = \gamma = 90°$.

The adducts of group 12 metal alkyls were studied in a pioneering series of papers by Thiele.[1-5] A range of nitrogenous bases were used including monodentate ligands such as trimethyl- and triethylamine and potentially chelating ligands such as 1,10-phenanthroline, the latter being also studied by Coates.[6] The adducts with monodentate ligands were generally low boiling point liquids; those with the chelating ligands, volatile solids. Adducts of both 1:1 and 2:1 stoichiometries were formed by the monodentate amines. The tendency of many of the 2:1 adducts to dissociate into 1:1 species, in solution, in nondonor solvents such as benzene, was noted on the basis of cryoscopic molecular weight measurements. Dissociation

(1) Thiele, K. H. *Z. Anorg. Allg. Chem.* **1962**, *319*, 183.
(2) Thiele, K. H. *Z. Anorg. Allg. Chem.* **1963**, *322*, 71.
(3) Thiele, K. H. *Z. Anorg. Allg. Chem.* **1963**, *325*, 156.
(4) Thiele, K. H. *Z. Anorg. Allg. Chem.* **1964**, *330*, 8.
(5) Thiele, K. H. *Z. Anorg. Allg. Chem.* **1968**, *325*, 156.

(6) Coates, G. E.; Green, S. I. E. *J. Chem. Soc.* **1962**, 3340.

0276-7333/91/2310-3196$02.50/0